Illuminating N-acylethanolamine biosynthesis with new chemical tools

Mock, E.D.

Chapter 2

High-throughput screening delivers new inhibitors for NAPE-PLD

2.1 Introduction

N-acylphosphatidylethanolamine phospholipase D (NAPE-PLD) is an enzyme that produces a family of bioactive signaling lipids called *N*-acylethanolamines (NAEs) from *N*-acylphosphatidylethanolamines (NAPEs). The enzyme has a metallo-β-lactamase fold and cannot perform transphosphatidylation, making it distinct from the PLD enzyme family.[1] A crystal structure of NAPE-PLD showed that the active site contains two Zn^{2+}-ions bridged by one hydrolytic water molecule, all coordinated by several histidine and aspartic acid residues (Figure 1A).[2]

The NAE products exert their biological effects through multiple protein classes, including G protein-coupled receptors (*e.g.* cannabinoid receptors type 1 and type 2, GPR55), ion channels (*e.g.* transient receptor potential vanilloid 1) and nuclear receptors (*e.g.* peroxisome proliferator-activated receptor (PPAR)-α) that are involved in a multitude of biological processes, such as neurotransmission, immunomodulation, energy balance, motor coordination, addiction, pain sensation, appetite, inflammation,

neurodegeneration and anxiety.[3] Better understanding of the physiological role of NAPE-PLD and the NAEs products has been hampered by a lack of pharmacological tools that allow acute modulation of the enzyme in live animals. These tools are essential to effectively perturb NAE signaling, as different NAPE-PLD knock-out (KO) mice studies have shown inconsistent results, with NAE levels not reduced in all cases, possibly due to long-term compensatory effects.[4-8]

So far, few inhibitors for NAPE-PLD have been reported. Out of a small library of NAPE substrate mimics, phosphoramidate AHP-71B was described as an inhibitor with micromolar potency (IC_{50} ~ 10 μM) (Figure 1B).[9] Other reported active compounds are β-lactamase substrate nitrocefin[9], desketoraloxifene analog 17b[10], which also targets phospholipase D1 (PLD1), and sulfonamide ARN19874[11]. All compounds showed poor to moderate potency for NAPE-PLD *in vitro*. Of note, ARN19874 was able to increase NAPE levels in HEK293 cells, but did not affect most NAE levels.[11] Therefore, new and more potent chemotypes are required to target NAPE-PLD *in vivo*.

Over the past three decades, the discovery of new first-in-class drugs has primarily relied on target-based approaches.[12] High-throughput screening (HTS) has been the predominant method for identifying new chemical entities, while fragment-based screening, virtual screening and structure-based design have also been successfully employed.[13] To start a HTS campaign a biochemical assay needs to be developed that allows the testing of 10,000 to 100,000 compounds per day.[14] Most of the currently available NAPE-PLD activity assays use thin-layer chromatography (TLC) or mass

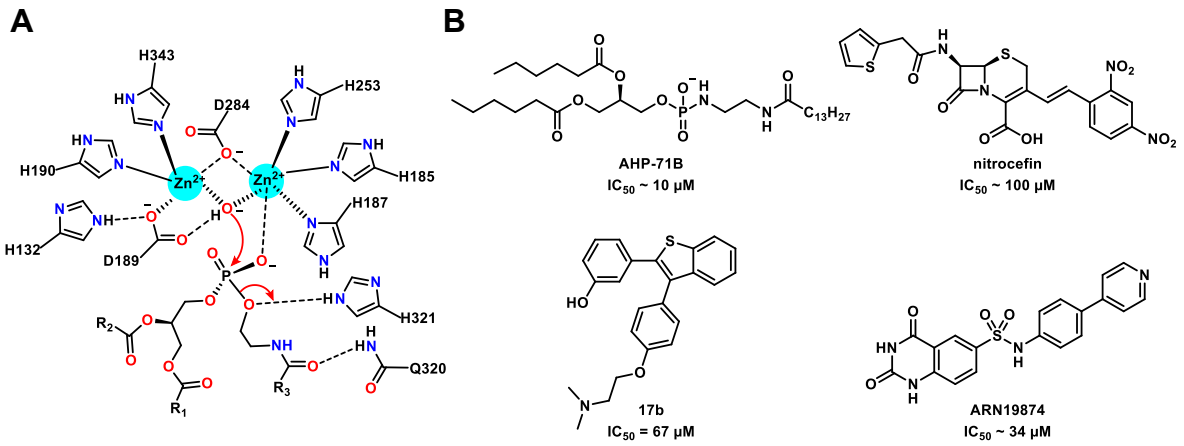

Figure 1. A) Model of the NAPE-PLD active site mechanism based on the published crystal structure.[2] **B**) Reported inhibitors for NAPE-PLD.

spectrometry (MS) as a read-out and are therefore not compatible with high-throughput screening.[1,4,11] In this chapter the optimization of a recently reported fluorescent NAPE-PLD activity assay[15] and its successful application in the screening of the Joint European Compound Library (JECL) as part of the European Lead Factory[16] (ELF) is described. Four new chemotypes were discovered of which the most promising scaffold was confirmed as a selective, submicromolar potent inhibitor for NAPE-PLD.

2.2 Results

A previously reported fluorescent NAPE-PLD activity assay[15] using the surrogate substrate *N*-((6-(2,4-dinitrophenyl)amino)hexanoyl)-2-(4,4-difluoro-5,7-dimethyl-4-bora-3a,4a-diaza-*s*-indacene-3-pentanoyl)-1-hexa-decanoyl-*sn*-glycero-3-phosphoethanolamine triethylammonium salt (PED6) was converted to a HTS-compatible format. The assay principle relies on the cleavage of the phosphodiester bond of PED6 by NAPE-PLD, thereby liberating the fluorescent BODIPY from the dinitroaniline quencher, which is proportional to the enzymatic activity (Figure 2A). Firstly, the assay was altered to accommodate membrane fractions of NAPE-PLD overexpressing cells as an enzyme source instead of purified NAPE-PLD. This circumvents the need for laborious protein purification. Human embryonic kidney (HEK293T) cells were transiently transfected with a pcDNA3.1 plasmid containing human NAPE-PLD-FLAG. After 72 hours the cells were lysed, membrane

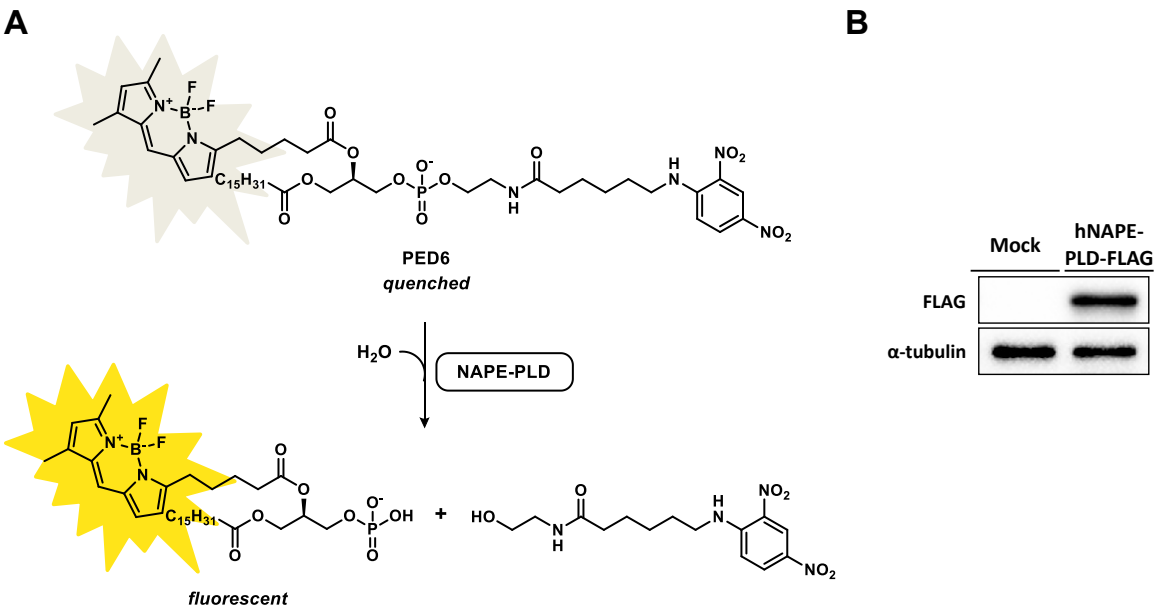

Figure 2. A) NAPE-PLD PED6 assay principle. **B**) Western blot of the membrane fraction from mock or hNAPE-PLD transfected HEK293T cells. α-Tubulin was used as a loading control.

fractions were prepared and the protein expression was confirmed by Western blot using anti-FLAG antibodies (Figure 2B).

Next, the optimal assay conditions were determined in a 96-well plate. The enzyme activity was linear between 0.01 and 0.5 μg/μL membrane lysate (Figure 3A). The signal-to-background (S/B)-ratio was determined between 0.02 and 0.05 μg/μL, minimizing the amount of lysate required, which gave 0.04 μg/μL as the optimal concentration (Figure 3B). The NAPE-PLD activity was highest at pH 7.5 (Figure 3C). Triton X-100 was employed as a rate enhancing non-ionic detergent[17-19], with optimal activity and S/B-ratio at 0.02% (v/v) (Figure 3D). Screening various salts showed that NaCl, KCl and $MgCl_2$ enhanced the enzymatic activity, giving an optimal 2.5-fold increase for 150 mM NaCl (Figure 3E). $ZnCl_2$ was inhibitory with an IC_{50} of 60 μM (95% confidence interval (CI): 46-78 μM), confirming previous findings for purified rat NAPE-PLD in a radioactive natural substrate assay.[19-21] Although purified NAPE-PLD has been reported to be stimulated by millimolar $CaCl_2$

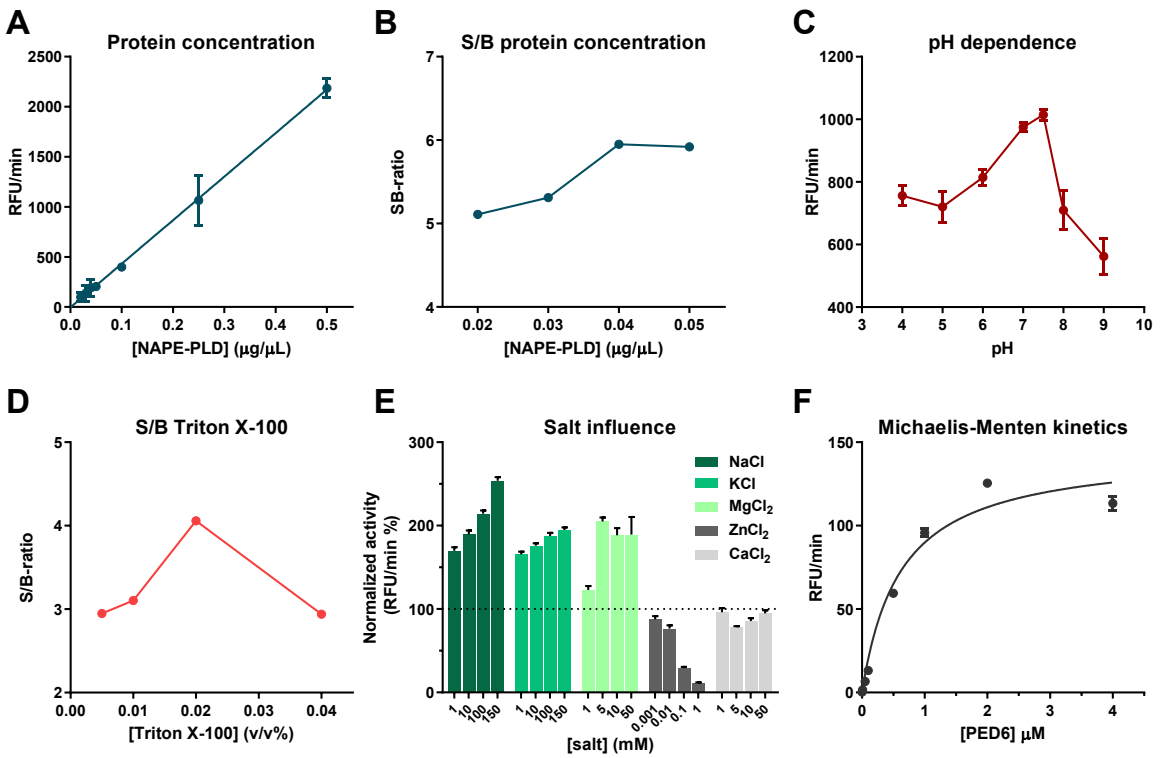

Figure 3. Optimization of the NAPE-PLD PED6 surrogate substrate assay. **A**) Protein concentration vs. enzyme rate was linear between 0.01 and 0.5 μg/μL. **B**) Optimal S/B-ratio at 0.04 μg/μL membrane lysate. **C**) Optimal enzyme activity at pH 7.5. **D**) Optimal S/B-ratio at 0.02% Triton X-100. **E**) NaCl (150 mM) increases the enzyme activity 2.5 fold. **F**) Michaelis-Menten plot (K_M = 0.59 ± 0.08 μM, V_{max} = 145 RFU/min). Data represent mean values ± SD (n = 2-4).

concentrations[20], in this assay $CaCl_2$ did not affect the NAPE-PLD activity. A prior study reported that the presence of phosphatidylethanolamine (PE) in the membrane fraction of NAPE-PLD transfected COS-7 cells constutively activate NAPE-PLD, thereby mitigating the Ca^{2+}-induced stimulatory effect.[21] A Michaelis-Menten constant (K_M) of 0.59 ± 0.08 μM was determined for PED6 using the optimized assay conditions (Figure 3F). The intra-plate variability of the assay, measured as the coefficient of variance (CV), was 3.3%. This indicated that the assay is robust and compatible for high-throughput screening, which according to the ELF screening requirements should be a CV < 10%.[22] Next, the assay was miniaturized to a 384-well format to allow compatibility with the ELF program. This afforded a S/B-ratio of 5.4 and statistical effect size Z' of 0.89, well within the ELF limits for a HTS-compatible assay (S/B-ratio > 3 and Z' > 0.6).[22]

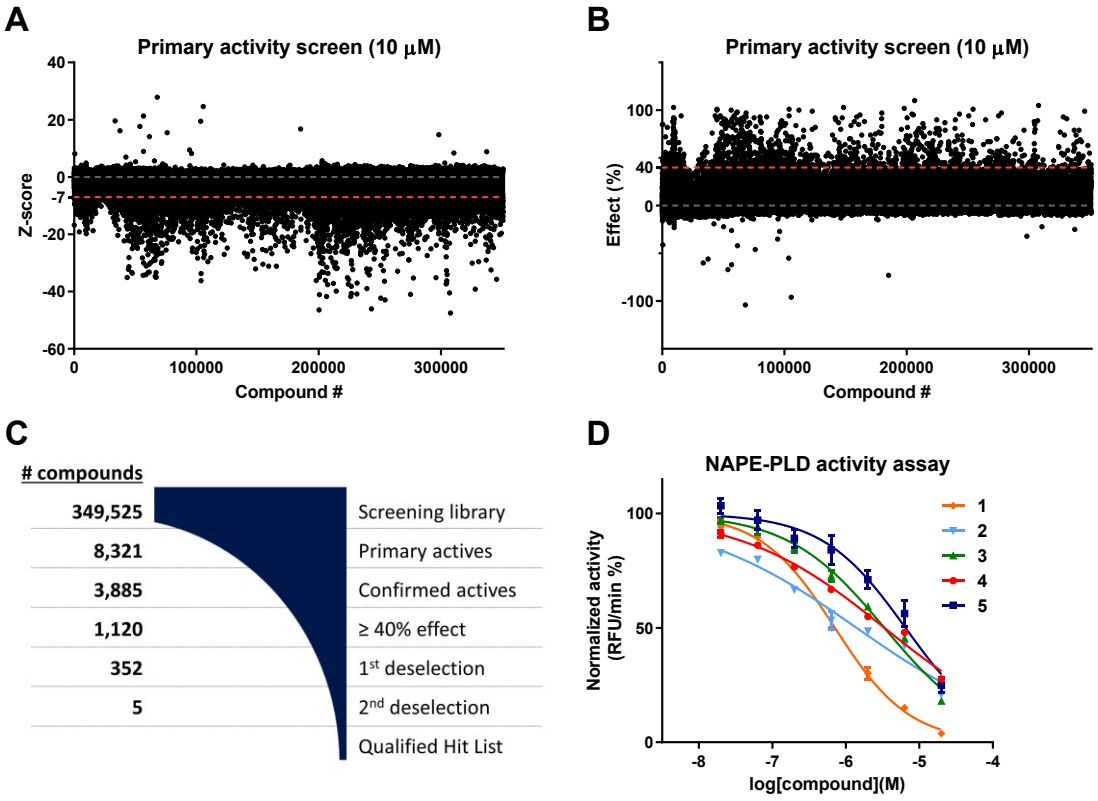

Figure 4. A) Primary activity screen plotted as Z-score. **B**) Primary activity screen plotted as effect %. **C**) Hit triage of the high-throughput campaign. **D**) Dose-response curves of hit compounds **1-5**. Data represent mean values ± SEM (n = 2).

Further assay miniaturization was performed by the Pivot Park Screening Centre to afford a 1,536-well assay. This resulted in a robust assay with Z' = 0.87, S/B-ratio = 6.7 and

CV = 3.3%. Approximately 350,000 compounds at a single concentration (10 μM) were screened in 294 plates in 3 days, affording 8321 actives using the cut-off value of Z-score ≤ -7 (> 20% -30% effect) (Figure 4A,C). Hit validation at the same concentration gave 3885 confirmed actives. To reduce the number of compounds, the percent effect on the enzyme activity (≥ 40%) was utilized to obtain a list of 1120 actives (Figure 4B,C). Next, dose-response curves were generated in the presence and absence of $ZnSO_4$ (100 μM) to remove promiscuous Zn^{2+}-ion chelators, which yielded 352 hits. $ZnCl_2$ demonstrated an IC_{50} of 60 μM (Figure 3E), however the S/B-ratio (8.2) and Z' (0.68) of the leftover NAPE-PLD activity was sufficient to obtain reliable dose-response curves. Visual inspection of the 352 compounds revealed the presence of potential assay interfering compounds that absorbed light within the visible wavelength, therefore a second deselection assay was

Table 1. NAPE-PLD activity and physicochemical parameters of HTS hit compounds **1-5**.

ID	Structure	pIC_{50} ± SEM	K_i (μM)	Desel. 1 pIC_{50} (+ $ZnSO_4$)	Desel. 2 pIC_{50} (quenching)	MW[a] (Da)	cLogP[b]	LipE[c]	tPSA[b] ($Å^2$)
1	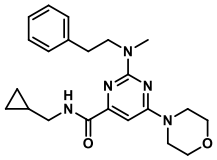	**6.14 ± 0.02**	0.26	6.15	<4.7	396	3.84	2.30	69.5
2	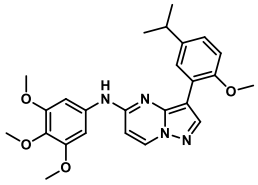	**5.86 ± 0.06**	0.51	5.44	4.73	449	4.63	1.23	76.9
3	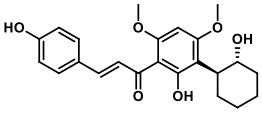	**5.46 ± 0.04**	1.3	5.21	5.08	398	3.42	2.04	96.2
4	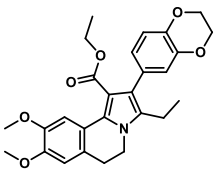	**5.48 ± 0.04**	1.2	5.62	<4.7	464	6.23	-0.75	66.5
5	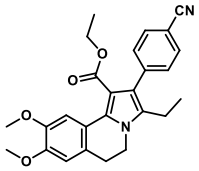	**5.20 ± 0.05**	2.3	5.14	<4.7	431	5.75	-0.55	71.8

[a] MW: molecular weight; [b] cLogP and topological polar surface area (tPSA) were calculated using Chemdraw 15; [c] Lipophilic efficiency (LipE) = pIC_{50} - cLogP.

developed. The substrate PED6 was incubated with lysate to obtain the maximum fluorescent signal, followed by incubation with different concentrations of the confirmed actives to determine the ability of the compounds to quench the fluorescent signal under the primary assay conditions. Only compounds that demonstrated no effect (pIC_{50} < 5) in the second deselection assay were selected. Notably, nitrocefin was identified as a false positive inhibitor using this procedure. The compounds were checked for purity (> 85%) and correct molecular weight (MW) by liquid chromatography-mass spectrometry (LC-MS) analysis. This afforded a qualified hit list of 5 compounds with four different chemotypes (Table 1, Figure 4D).

Compound **1** (*N*-(cyclopropylmethyl)-2-(methyl(phenethyl)amino)-6-morpholino-pyrimidine-4-carboxamide) displayed the most optimal biological and physicochemical characteristics (MW = 396, cLogP = 3.84, LipE = 2.30) (Table 2). Resynthesis of **1** was achieved by chlorination of orotic acid **6**, followed by three sequential chemoselective substitution reactions with cyclopropylmethanamine, morpholine and *N*-methylphenethylamine, respectively, affording **1** (Scheme 1). After chemical analysis and retesting in the NAPE-PLD activity assay, the identity and submicromolar potency (pIC_{50} ± SE = 6.09 ± 0.04, K_i = 0.30 μM, 95% CI = 0.22 - 0.38 μM) of hit compound **1** was confirmed.

Subsequently, the selectivity of **1** for the proteins of the endocannabinoid system was evaluated. Compound **1** did not show any significant inhibitory activities at 10 μM at the cannabinoid receptors type 1 and type 2 (Table 2) as well as for the other proteins involved in anandamide biosynthesis and degradation, such as phospholipase A2 group 4E (PLA2G4E) and fatty acid amide hydrolase (FAAH), respectively (Table 3, Figure 5). Furthermore, **1** did not inhibit the enzymes involved in the biosynthesis and degradation of the endocannabinoid 2-arachidonoylglycerol (2-AG), including diacylglycerol lipases (DAGLα/β), monoacylglycerol lipase (MAGL) and α,β-hydrolase domain containing 6 (ABHD6) (Table 3, Figure 5).

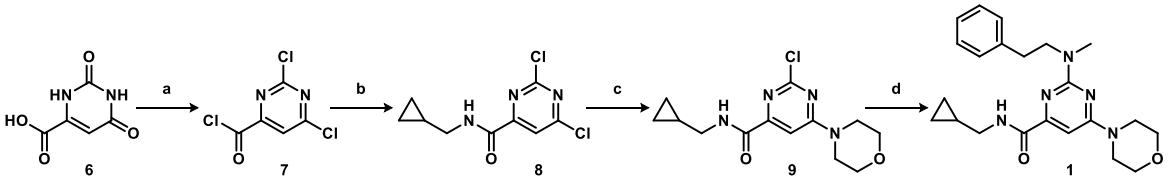

Scheme 1. Synthesis of hit compound **1**. Reagents and conditions: a) $POCl_3$, DMF, reflux, 60%; b) cyclopropylmethanamine, Et_3N, DCM, -78 °C to 0 °C, 80%; c) morpholine, DiPEA, MeOH, 0 °C, 89%; d) *N*-methylphenethylamine, DiPEA, n-BuOH, μW, 160 °C, 50%.

Table 2. **1** shows no significant inhibitory activity for the CB_1 and CB_2 receptors.

Radioligand displacement at 10 μM 1 (% ± SD)	
hCB_1	hCB_2
39 ± 6	40 ± 6

>50% is considered a target

Table 3. No inhibitory activities were found for **1** for the metabolic enzymes of the ECS. Activities were measured using surrogate or natural substrate assays for DAGLα/β and MAGL, or activity-based protein profiling for PLA2G4E.

Remaining enzyme activity at 10 μM 1 (% ± SD)			
hDAGLα	mDAGLβ	hMAGL	hPLA2G4E
103 ± 9	86 ± 13	74 ± 7	118 ± 17

< 50% is considered a target.

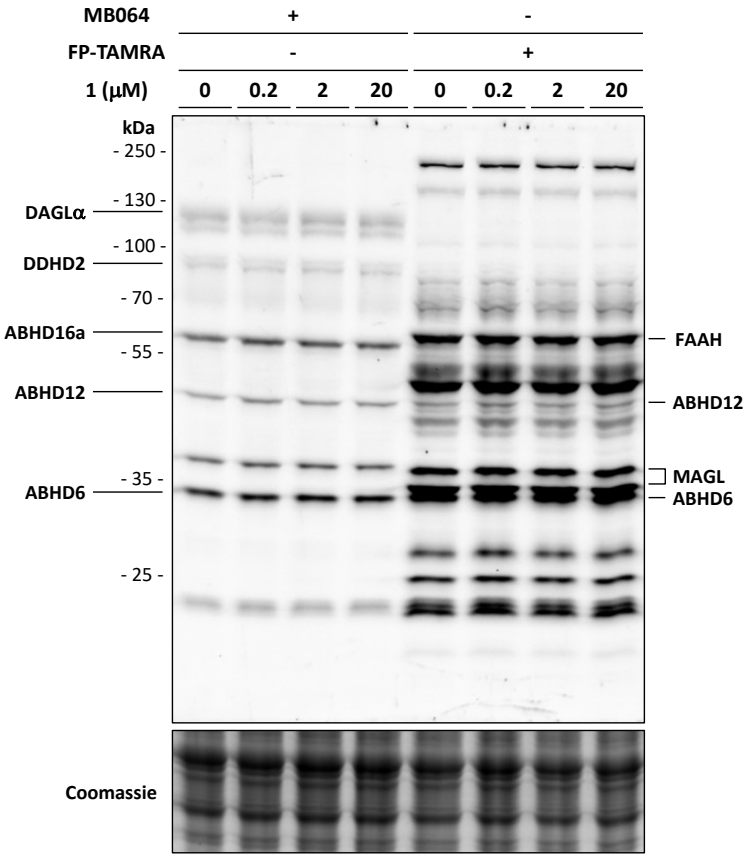

Figure 5. Competitive activity-based protein profiling of **1** in mouse brain membrane fractions using broad-spectrum lipase probes MB064[23] (0.25 μM) and FP-TAMRA (0.5 μM). No probe targets were competed by **1**. Structures of MB064 and FP-TAMRA in Supplementary Figure 1.

2.3 Conclusion

In this chapter, the succesful optimization of a NAPE-PLD fluorescent surrogate substrate assay and high-throughput screening of the Joint European Compound Library is described. This provided five hits from four new chemotypes: two dihydropyrrolo[2,1-a]isoquinoline-1-carboxylate esters and three singletons. On the basis of its favorable potency and physicochemical properties, pyrimidine-4-carboxamide **1** was selected for resynthesis. The submicromolar activity of **1** could be confirmed, making it the most potent NAPE-PLD inhibitor to date. In addition, **1** was selective over the receptors and enzymes of the endocannabinoid system. It is anticipated that these new chemical scaffolds, in particular compound **1**, may provide a useful starting point for the discovery of *in vivo* active NAPE-PLD inhibitors.

Acknowledgements

The research leading to these results has received support from the Innovative Medicines Initiative Joint Undertaking under grant agreement n°115489, resources of which are composed of financial contribution from the European Union's Seventh Framework Programme (FP7/2007-2013) and EFPIA companies. Anouk van der Gracht and Ioli Kotsogianni are kindly acknowledged for their contributions with regard to the NAPE-PLD assay development and compound synthesis. Marjolein Soethoudt, Ming Jiang, Tom van der Wel, Timo Wendel and Anthe Janssen are acknowlegded for performing biochemical assays. Jesse Wat, Helma van den Hurk, Stan van Boeckel and the Pivot Park Screening Centre are kindly acknowledged for conducting the high-throughput screen.

2.4 Experimental Methods

A. Biological Procedures

Cloning of plasmid DNA

Full length human cDNA of human NAPE-PLD (obtained from Natsuo Ueda[1]), hDAGLα, mDAGLβ, hMAGL and hPLA2G4E was cloned into mammalian expression vector pcDNA3.1, containing a C-terminal FLAG-tag and genes for ampicillin and neomycin resistance. All plasmids were grown in XL-10 Z-competent cells and prepped (Maxi Prep, Qiagen). Constructs were verified by Sanger sequencing (Macrogen).

Cell culture

HEK293T were cultured at 37 ^{o}C and 7% CO_2 in DMEM (Sigma Aldrich, D6546) with GlutaMax (2 mM), penicillin (100 μg/ml, Duchefa), streptomycin (100 μg/ml, Duchefa) and 10% newborn calf serum (Thermo Fisher). Cells were passaged twice a week to appropriate confluence by thorough pipetting.

Transient transfection

One day before transfection 10^7 cells were seeded in 15 cm petri dishes. Two hours before transfection the medium was refreshed with 13 mL medium. Transfection was performed with polyethyleneimine (PEI, 60 μg per dish) in a ratio of 3:1 with plasmid DNA (20 μg per dish). PEI and plasmid DNA were incubated in serum free medium (2 mL per dish) at rt for 15 min, followed by dropwise addition to the cells. Transfection with the empty pcDNA3.1 vector was used to generate mock control samples. The medium was refreshed after 24 hours and cells were harvested after 48 or 72 hours in cold PBS. Cells were centrifuged (10 min, 200 *g*, 4 ^{o}C) and the supernatant was removed. The cell pellets were flash frozen in liquid N_2 and stored at -80 ^{o}C.

Cell lysate preparation

Cell pellets were resuspended in lysis buffer: 20 mM HEPES pH 7.2, 2 mM DTT, 0.25 M sucrose, 1 mM $MgCl_2$, 2.5 U/mL benzonase and incubated on ice for 30 minutes. The cells were homogenized with a Heidolph SilentCrusher S (5F, 20,000 rpm, 3 x 7s). The cytosolic fraction (supernatant) was separated from the membranes by ultra-centrifugation (30 min, 100,000 *g*, 4 ^{o}C, Beckman Coulter, Ti 70.1 rotor). The pellet (membrane fraction) was resuspended in storage buffer (20 mM HEPES pH 7.2, 2 mM DTT) and homogenized with a Heidolph SilentCrusher S (5F, 20,000 rpm, 3 x 7s). Protein concentrations were determined using a Quick Start™ Bradford protein assay (Bio-Rad). All samples were stored at -80 ^{o}C.

Mouse brain lysate preparation

Mouse brain lysate was prepared as described previously.[24] Mouse brains (C57BL/6) were isolated according to guidelines approved by the ethical committee of Leiden University (DEC#13191), frozen in liquid N_2 and stored at -80 ^{o}C. Tissues were thawed on ice, dounce homogenized in cold lysis buffer (20 mM HEPES pH 7.2, 2 mM DTT, 1 mM $MgCl_2$, 25 U/mL benzonase) and incubated on ice (15 min), followed by low-speed centrifugation (2,500 *g*, 3 min, 4 ^{o}C) to remove debris. After high-speed centrifugation (100,000 *g*, 45 min, 4 ^{o}C) the supernatant was collected as the cytosol fraction. The pellet was resuspended in cold storage buffer (20 mM HEPES pH 7.2, 2 mM DTT). Protein concentrations were determined by a Quick Start™ Bradford protein assay (Bio-Rad) or Qubit™ protein assay (Invitrogen). Samples were flash frozen in liquid N_2 and stored at -80 ^{o}C.

Western blot

Cell lysates were denatured with 4x Laemmli buffer (stock concentrations: 240 mM Tris-HCl pH 6.8, 8% w/v SDS, 40% v/v glycerol, 5% v/v β-mercaptoethanol, 0.04% v/v bromophenol blue, 30 min, RT) and 10-20 μg per sample was resolved on a 10% acrylamide SDS-PAGE gel (180 V, 75 min). Proteins were transferred from the gel to a 0.2 μm PVDF membrane using a Trans-Blot® Turbo (Bio-Rad). The membranes were washed with TBS (50 mM Tris-HCl pH 7.5, 150 mM NaCl) and blocked with 5% milk in TBST (50 mM Tris-HCl pH 7.5, 150 mM NaCl, 0.05% Tween 20) 1 h at rt or overnight at 4 ^{o}C. Primary antibodies against FLAG-tagged proteins (Sigma Aldrich, F3165, 1:5000 in 5% milk in TBST) or α-tubulin (Genetex, GTX76511, 1:5000 in 5% milk in TBST) were incubated 1 h at rt or overnight at 4 ^{o}C. Membranes were washed with TBST and incubated with secondary antibodies: for FLAG-tagged proteins, goat-anti-mouse-HRP (Santa Cruz, sc-2005, 1:5000 in 5% milk in TBST); for α-tubulin, goat-anti-rat (Santa Cruz, sc-2032, 1:5000 in 5% milk in TBST). All secondary antibodies were incubated for 1 h at rt. Membranes were washed with TBST and TBS. The blot was developed in the dark using a luminal solution (10 mL, 1.4 mM luminal in Tris-HCl pH 8.8), ECL enhancer (100 μL, 6.7 mM *para*-hydroxycoumaric acid in DMSO) and H_2O_2 (3 μL, 30% w/w in H_2O). Chemiluminescence was visualized using a ChemiDoc™ Imaging System (Bio-Rad). Band intensity is normalized to α-tubulin using ImageLab software (Bio-Rad).

Surrogate substrate-based fluorescence assay NAPE-PLD

The NAPE-PLD activity assay was based on a previously reported method with small alterations.[15] The membrane fraction from transient overexpression of human NAPE-PLD in HEK293T cells was diluted to 0.4 μg/μL in assay buffer (50 mM Tris-HCl pH 7.5, 150 mM NaCl, 0.02% Triton X-100). The substrate PED6

(Invitrogen, D23739) 1 mM stock in DMSO was consecutively diluted in DMSO (10x) and in assay buffer (10x) to make a 10 μM working solution. Relevant concentrations of compound (100x working solution) were prepared in DMSO. The assay was performed in a dark Greiner 96-well plate (flat bottom), final volume 100 μL. The compound or DMSO was incubated with membrane protein lysate (final concentration 0.04 μg/μL) for 30 minutes at 37 °C. Then, substrate PED6 was added (final concentration 1 μM) and the measurement was started immediately on a TECAN infinite M1000 pro at 37 °C (excitation 485 nm, emission 535 nm, gain = 100), scanning every 2 minutes for 1 h. Mock membrane lysate with DMSO was used for background subtraction. The slope of t = 4 min to t = 14 min was used as the enzymatic rate (RFU/min), which was normalized to generate IC_{50} curves using Graphpad Prism v6 (log(inhibitor) vs. normalized response with variable slope). K_i values were calculated from the Cheng-Prusoff equation $K_i = IC_{50}/(1+([S]/K_M))$ where K_M = 0.59 μM. All measurements were performed in N = 2, n = 2 or N = 2, n = 4 for controls, with Z' ≥ 0.6.

High-throughput screening of NAPE-PLD activity assay

High-throughput screening of the NAPE-PLD activity assay was performed at Pivot Park Screening Centre B.V. Assay buffer with Triton-X100 (prepared on the day of the assay): 1x assay buffer (50 mM Tris-HCl pH 7.5, 150 mM NaCl, 0.02% Triton-X100 (Sigma-Aldrich)). In a black 1536-well plate (Corning, Cat# 3724, Lot# 19214025) was added 10 nL of 4 mM compound (final compound concentration 10 μM and final DMSO concentration 0.25%). 10 nL of DMSO was added to the min wells or 10 nL of 40 mM nitrocefin (Millipore) to the max wells (final nitrocefin concentration 100 μM and final DMSO concentration 0.25%). 2 μL of 0.08 μg/μL hNAPE-PLD membrane lysate in assay buffer was added (final concentration 0.04 μg/μL), followed by incubation for 30 minutes at rt. Then 2 μL of 1 μM PED6 in assay buffer (final concentration 0.5 μM) was added and the plate was incubated for 1 h at rt. Fluorescence intensity signal (excitation 485 nm, emission 535 nm) was measured on a Envision reader. For dispensing an Echo-555 was used for 10 nL compounds, nitrocefin or DMSO. A Multidrop Combi was used for dispensing 2 μL hNAPE-PLD lysate and a BioRAPTR for dispensing 2 μL PED6. In this manner the Joint European Compound Library (JECL) consisting of 349,525 compounds was screened in 294 plates with a S/B ratio between 5.48-7.08 and Z' between 0.66-0.91. As a hit criterium a Z-score ≤ -7 was used (Z-score = $(X - \mu)/\sigma$ where X = measured effect, μ = mean effect, σ = standard deviation). This gave a hit rate of 2.4% (8,321 primary actives). The primary actives were screened again at 10 μM (single point) giving 3,885 confirmed actives. Due to the large number of compounds the cut-off score was changed to ≥ 40 effect %, giving 1,120 hits. Dose-response curves (7 equidistant concentration steps from 20 μM to 20 nM, n = 2) were performed with or without 100 μM $ZnSO_4$ to remove promiscuous zinc chelators, which gave 352 compounds. A second deselection to remove fluorescence quenchers was performed: first the maximum fluorescence signal was obtained by incubating PED6 with hNAPE-PLD membrane lysate, then the compounds were added in a similar dose-response concentration curve (n = 2). Five compounds (**1-5**) demonstrating no effect ($pIC_{50} < 5$) in the second deselection assay were selected (Table 1).

Natural substrate-based fluorescence assay DAGLα

The hDAGLα natural substrate assay was performed as reported previously.[25] Standard assay conditions: 0.2 U/mL glycerol kinase (GK), glycerol-3-phosphate oxidase (GPO) and horseradish peroxidase (HRP), 0.125 mM ATP, 10 μM Amplifu™Red, 5% DMSO in a total volume of 200 μL. The assay additionally contained 5 μg/mL hMAGL overexpressing membranes, 100 μM SAG and 0.0075% (w/v) Triton X-100, with a final protein concentration of 50 μg/mL. All measurements were performed in N = 2, n = 2 or N = 2, n = 4 for controls, with Z' ≥ 0.6.

Surrogate substrate-based fluorescence assay DAGLβ

The biochemical mDAGLβ assay was performed as reported previously.[23] In brief, the biochemical mDAGLβ activity assay is based on the hydrolysis of *para*-nitrophenylbutyrate (PNP-butyrate) by membrane preparations from HEK293T cells transiently transfected with mDAGLβ. Reactions were performed in 50 mM

HEPES pH 7.2 buffer with 0.05 μg/μL mDAGLβ transfected membrane fractions (final protein concentration). All measurements were performed in N = 2, n = 2 or N = 2, n = 4 for controls, with Z' ≥ 0.6.

Natural substrate-based fluorescence assay MAGL

The MAGL activity assay is based on the production of glycerol from 2-arachidonoylglycerol (2-AG) hydrolysis by hMAGL overexpressing membrane preparations from transiently transfected HEK293T cells, as previously reported.[26] Glycerol is formed during the reaction and is coupled to the oxidation of commercially available Amplifu™Red via a multi-enzyme cascade, resulting in a fluorescent signal from resorufin. Standard assays were performed in HEMNB buffer (50 mM HEPES pH 7.4, 1 mM EDTA, 5 mM $MgCl_2$, 100 mM NaCl, 0.5% w/v BSA) in black, flat bottom 96-wells plates. Final protein concentration of membrane preparations from overexpressing hMAGL HEK293T cells was 1.5 μg/mL (0.3 μg per well). Inhibitors were added from 40x concentrated DMSO stocks. After 20 min incubation, 100 μL assay mix containing glycerol kinase (GK), glycerol-3-phosphate oxidase (GPO), horse radish peroxidase (HRP), adenosine triphosphate (ATP), Amplifu™Red and 2-arachidonoylglycerol (2-AG) was added and fluorescence was measured in 5 min intervals for 60 min on a plate reader. Final assay concentrations: 0.2 U/mL GK, GPO and HRP, 0.125 mM ATP, 10 μM Amplifu™Red, 25 μM 2-AG, 5% DMSO, 0.5% ACN in a total volume of 200 μL. All measurements were performed in N = 2, n = 2 or N = 2, n = 4 for controls, with Z' ≥ 0.6. For IC_{50} determination, slopes of corrected fluorescence in time were determined in the linear interval of t = 10 to t = 35 min and then scaled to the corrected positive control of hMAGL-overexpressing membranes treated with vehicle (DMSO) as a 100% activity reference point. The data was exported to GraphPad Prism v6 and analyzed in a non-linear dose-response analysis with variable slope.

Radioligand displacement assays CB_1 and CB_2 receptor

[^{3}H]CP55940 displacement assays to determine the affinity for the cannabinoid CB_1 and CB_2 were performed as previously described.[27] Membrane aliquots containing 5 μg (CHOK1hCB_1_bgal) or 1.5 μg (CHOK1hCB_2_bgal) of membrane protein were incubated in a total volume of 100 μL assay buffer (50 mM Tris-HCl pH 7.4, 5 mM $MgCl_2$ and 0.1% BSA) at 25 °C for 2 hours in presence of ~3 nM or ~1.5 nM [^{3}H]CP55940, respectively. NAPE-PLD inhibitors were added at 50, 10 or 1 μM (final concentration) and nonspecific binding was determined in the presence of 10 μM rimonabant (CHOK1hCB_1_bgal) or 10 μM AM630 (CHOK1hCB_2_bgal). Incubations were terminated by harvesting the samples on 96-well GF/C filters, precoated with 25 μL 0.25% (v/v) PEI per well, with rapid vacuum filtration, to separate the bound and free radioligand, using a Perkin Elmer 96-well harvester (Perkin Elmer, Groningen, The Netherlands). Filters were subsequently washed ten times with ice-cold assay buffer on the 96-well plate and 5 times on a wash plate. Filter plates were dried at 55 °C for ~45 min, then 25 μL Microscint was added per well (Perkin Elmer, Groningen, The Netherlands). After 3 hours, the filter-bound radioactivity was determined by scintillation spectrometry using a Microbeta2® 2450 microplate counter (Perkin Elmer, Boston, MA).

Activity based protein profiling for FAAH, ABHD6, ABHD12 and PLA2G4E activity

Gel-based activity based protein profiling (ABPP) was performed as previously described.[23] In brief, mouse brain membrane proteome or hPLA2G4E overexpressing cytosol lysate (9.5 μL, 2 or 1 μg/μL, respectively) was pre-incubated with vehicle or inhibitor (0.5 μL 40x inhibitor stock in DMSO, 30 min, rt) followed by incubation with the activity based probe MB064 (250 nM, prepared in house) or FP-TAMRA (500 nM, Invitrogen) for mouse brain lysate (15 min, rt) or FP-TAMRA (50 nM) for PLA2G4E overexpressing lysate (5 min, rt). Final concentrations for the inhibitors are indicated in the main text and figure legends. Proteins were denatured with 4x Laemmli buffer (3.5 μL, stock concentrations: 240 mM Tris-HCl pH 6.8, 8% w/v SDS, 40% v/v glycerol, 5% v/v β-mercaptoethanol, 0.04% v/v bromophenol blue, 30 min, rt). The samples (10 μL per slot) were resolved by SDS-PAGE (respectively, 10% or 8% acrylamide for mouse brain or PLA2G4E lysate, 180 V, 75 min). Gels were scanned using Cy3 and Cy5 multichannel settings (605/50 and 695/55

filters, respectively) on a ChemiDoc™ Imaging System (Bio-Rad). Fluorescence was normalized to Coomassie staining and quantified with Image Lab (Bio-Rad).

B. Synthetic Procedures

General

All chemicals (Sigma-Aldrich, Fluka, Acros, Merck, Combi-Blocks, Fluorochem, TCI) were used as received. All solvents used for reactions were of analytical grade. THF, Et_2O, DMF, CH_3CN and DCM were dried over activated 4 Å molecular sieves, MeOH over 3 Å molecular sieves. Flash chromatography was performed on silica gel (Screening Devices BV, 40-63 μm, 60 Å). The eluent EtOAc was of technical grade and distilled before use. Reactions were monitored by thin layer chromatography (TLC) analysis using Merck aluminium sheets (Silica gel 60, F_{254}). Compounds were visualized by UV-absorption (254 nm) and spraying for general compounds: $KMnO_4$ (20 g/L) and K_2CO_3 (10 g/L) in water, or for amines: ninhydrin (0.75 g/L) and acetic acid (12.5 mL/L) in ethanol, followed by charring at ~150 °C. ^1H and ^{13}C NMR experiments were recorded on a Bruker AV-400 (400/101 MHz), Bruker DMX-400 (400/101 MHz) and Bruker AV-500 (500/126 MHz). Chemical shifts are given in ppm (δ) relative to tetramethylsilane or $CDCl_3$ as internal standards. Multiplicity: s = singlet, br s = broad singlet, d = doublet, dd = doublet of doublet, t = triplet, q = quartet, p = pentet, m = multiplet. Coupling constants (*J*) are given in Hz. LC-MS measurements were performed on a Thermo Finnigan LCQ Advantage MAX ion-trap mass spectrometer (ESI^+) coupled to a Surveyor HPLC system (Thermo Finnigan) equipped with a standard C18 (Gemini, 4.6 mm D x 50 mm L, 5 μm particle size, Phenomenex) analytical column and buffers A: H_2O, B: CH_3CN, C: 0.1% aq. TFA. High resolution mass spectra were recorded on a LTQ Orbitrap (Thermo Finnigan) mass spectrometer or a Synapt G2-Si high definition mass spectrometer (Waters) equipped with an electrospray ion source in positive mode (source voltage 3.5 kV, sheath gas flow 10 mL min-1, capillary temperature 250 °C) with resolution R = 60000 at m/z 400 (mass range m/z = 150-2000) and dioctylphtalate (m/z = 391.28428) as a lock mass. Preparative HPLC was performed on a Waters Acquity Ultra Performance LC with a C18 column (Gemini, 150 x 21.2 mm, Phenomenex). All final compounds were determined to be >95% pure by integrating UV intensity recorded via HPLC.

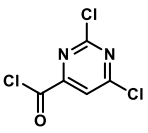

2,6-Dichloropyrimidine-4-carbonyl chloride (7). In a 500 mL round bottom flask orotic acid (15.6 g, 100 mmol, 1 eq) was dissolved in phosphorous oxychloride (46 mL, 500 mmol, 5 eq) and 10 drops of DMF were added. The mixture was heated to reflux and stirred for 19 h. *n*-Hexane (250 mL) was added and the mixture was stirred vigorously for 10 min and then transferred to a separatory funnel containing 100 mL H_2O. The flask was washed with 50 mL hexane. After shaking, the aqueous layer was removed and the hexane was washed with brine (1 x 100 mL), dried with $MgSO_4$ and concentrated under reduced pressure to yield the product (12.8 g, 60.4 mmol, 60%). ^1H NMR (500 MHz, $CDCl_3$) δ 8.00 (s, 1H). ^{13}C NMR (126 MHz, $CDCl_3$) δ 167.17, 165.27, 161.56, 158.19, 119.70.

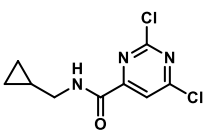

2,6-Dichloro-*N*-(cyclopropylmethyl)pyrimidine-4-carboxamide (8). A round bottom flask was charged with 2,6-dichloropyrimidine-4-carbonyl chloride **7** (0.63 mL, 5.0 mmol, 1 eq) and dry DCM (50 mL) and cooled to -78 °C. Et_3N (0.91 mL, 6.5 mmol, 1.3 eq) and cyclopropylmethanamine (0.44 mL, 5.1 mmol, 1.025 eq) were added and the mixture was stirred for 3.5 h while letting the acetone bath warm up to 0 °C. The mixture was transferred to a separatory funnel and the organic layer was washed with H_2O (2 x 50 mL) and brine (1 x 75 mL), dried (Na_2SO_4), filtered and concentrated under reduced pressure. Silica gel column chromatography (5% -> 20% EtOAc/pentane) afforded the product (0.99 g, 4.0 mmol, 80%). TLC: R_f = 0.8 (20% EtOAc/pentane). ^1H NMR (400 MHz, $CDCl_3$) δ 8.11 (s, 1H), 7.96 (br s, 1H), 3.44 – 3.27 (m, 2H), 1.20 – 1.03 (m, 1H), 0.68 – 0.52 (m, 2H),

0.32 (q, *J* = 4.8 Hz, 2H). ^{13}C NMR (101 MHz, $CDCl_3$) δ 164.74, 160.44, 160.04, 159.77, 118.22, 44.72, 10.57, 3.67. HRMS $[C_9H_{10}Cl_2N_3O + H]^+$: 246.0195 calculated, 246.0196 found.

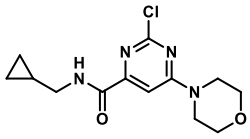

2-Chloro-*N*-(cyclopropylmethyl)-6-morpholinopyrimidine-4-carboxamide (9). A round bottom flask was charged with dichloropyrimidine **8** (1.7 g, 7.1 mmol, 1 eq) and dry MeOH (71 mL) and cooled to 0 °C. DiPEA (1.9 mL, 11 mmol, 1.5 eq) and morpholine (0.64 mL, 7.4 mmol, 1.05 eq) were added and the mixture was stirred for 2 h at 0 °C. The solvents were evaporated under reduced pressure and the crude material was purified by silica gel column chromatography (30% -> 60% EtOAc/pentane), affording the product (1.7 g, 6.3 mmol, 89%). R_f = 0.5 in 40% EtOAc/pentane. ^{1}H NMR (400 MHz, $CDCl_3$) δ 7.94 (t, *J* = 5.9 Hz, 1H), 7.28 (s, 1H), 3.87 – 3.63 (m, 8H), 3.33 – 3.25 (m, 2H), 1.12 – 1.00 (m, 1H), 0.61 – 0.52 (m, 2H), 0.32 – 0.24 (m, 2H). ^{13}C NMR (101 MHz, $CDCl_3$) δ 163.83, 162.21, 159.84, 157.90, 99.36, 66.35, 44.45, 10.65, 3.64. Regioselectivity was confirmed by NOESY analysis. HRMS $[C_{13}H_{17}ClN_4O_2 + H]^+$: 297.1113 calculated, 297.1116 found.

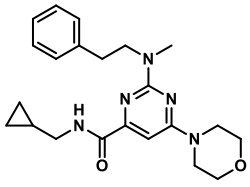

***N*-(Cyclopropylmethyl)-2-(methyl(phenethyl)amino)-6-morpholino-pyrimidine-4-carboxamide (1).** A microwave vial with a magnetic stir bar was charged with 2-chloropyrimidine **9** (59 mg, 0.20 mmol, 1 eq), *N*-methylphenethylamine hydrobromide (66 mg, 0.30 mmol, 1.5 eq), DiPEA (140 μL, 0.80 mmol, 4 eq) and *n*-BuOH (1 mL). The tube was capped, flushed with N_2 and heated to 160 °C in a microwave reactor (Biotage, 75 W) for 8 h. The reaction showed complete conversion as measured by LC/MS. The mixture was transferred to a round-bottom flask, concentrated under reduced pressure and coevaporated with toluene (2x). The residue was purified by silica gel column chromatography (40% -> 60% EtOAc/pentane), affording the product (40 mg, 0.10 mmol, 50%). TLC: R_f = 0.3 (40% EtOAc/pentane). ^{1}H NMR (400 MHz, $CDCl_3$) δ 8.03 (br s, 1H), 7.34 – 7.25 (m, 2H), 7.25 – 7.12 (m, 3H), 6.72 (s, 1H), 3.88 – 3.72 (m, 6H), 3.72 – 3.55 (m, 4H), 3.30 (t, *J* = 6.5 Hz, 2H), 3.13 (s, 3H), 2.90 (t, *J* = 7.7 Hz, 2H), 1.14 – 0.99 (m, 1H), 0.64 – 0.44 (m, 2H), 0.38 – 0.19 (m, 2H). ^{13}C NMR (101 MHz, $CDCl_3$) δ 164.66, 163.97, 160.86, 156.78, 139.92, 128.95, 128.58, 126.29, 90.08, 66.74, 51.68, 44.50, 44.11, 35.70, 33.93, 10.88, 3.48. HRMS $[C_{22}H_{29}N_5O_2 + H]^+$: 396.2394 calculated, 396.2387 found.

References

1. Okamoto, Y., Morishita, J., Tsuboi, K., Tonai, T. & Ueda, N. Molecular characterization of a phospholipase D generating anandamide and its congeners. *Journal of Biological Chemistry* **279**, 5298-5305 (2004).
2. Magotti, P., Bauer, I., Igarashi, M., Babagoli, M., Marotta, R., Piomelli, D. & Garau, G. Structure of human *N*-acylphosphatidylethanolamine-hydrolyzing phospholipase D: regulation of fatty acid ethanolamide biosynthesis by bile acids. *Structure* **23**, 598-604 (2015).
3. Hussain, Z., Uyama, T., Tsuboi, K. & Ueda, N. Mammalian enzymes responsible for the biosynthesis of *N*-acylethanolamines. *Biochimica et Biophysica Acta (BBA) - Molecular and Cell Biology of Lipids* **1862**, 1546-1561 (2017).
4. Leung, D., Saghatelian, A., Simon, G.M. & Cravatt, B.F. Inactivation of *N*-acyl phosphatidylethanolamine phospholipase D reveals multiple mechanisms for the biosynthesis of endocannabinoids. *Biochemistry* **45**, 4720-4726 (2006).
5. Simon, G.M. & Cravatt, B.F. Endocannabinoid biosynthesis proceeding through glycerophospho-*N*-acyl ethanolamine and a role for α/β-hydrolase 4 in this pathway. *Journal of Biological Chemistry* **281**, 26465-26472 (2006).

6. Simon, G.M. & Cravatt, B.F. Characterization of mice lacking candidate *N*-acyl ethanolamine biosynthetic enzymes provides evidence for multiple pathways that contribute to endocannabinoid production *in vivo*. *Molecular BioSystems* **6**, 1411-1418 (2010).
7. Tsuboi, K., Okamoto, Y., Ikematsu, N., Inoue, M., Shimizu, Y., Uyama, T., Wang, J., Deutsch, D.G., Burns, M.P., Ulloa, N.M., Tokumura, A. & Ueda, N. Enzymatic formation of *N*-acylethanolamines from *N*-acylethanolamine plasmalogen through *N*-acylphosphatidylethanolamine-hydrolyzing phospholipase D-dependent and -independent pathways. *Biochimica et Biophysica Acta (BBA) - Molecular and Cell Biology of Lipids* **1811**, 565-577 (2011).
8. Leishman, E., Mackie, K., Luquet, S. & Bradshaw, H.B. Lipidomics profile of a NAPE-PLD KO mouse provides evidence of a broader role of this enzyme in lipid metabolism in the brain. *Biochimica et Biophysica Acta (BBA) - Molecular and Cell Biology of Lipids* **1861**, 491-500 (2016).
9. Petersen, G., Pedersen, A.H., Pickering, D.S., Begtrup, M. & Hansen, H.S. Effect of synthetic and natural phospholipids on *N*-acylphosphatidylethanolamine-hydrolyzing phospholipase D activity. *Chemistry and Physics of Lipids* **162**, 53-61 (2009).
10. Scott, S.A., Spencer, C.T., O'Reilly, M.C., Brown, K.A., Lavieri, R.R., Cho, C.-H., Jung, D.-I., Larock, R.C., Brown, H.A. & Lindsley, C.W. Discovery of desketoraloxifene analogues as inhibitors of mammalian, Pseudomonas aeruginosa, and NAPE phospholipase D enzymes. *ACS Chemical Biology* **10**, 421-432 (2015).
11. Castellani, B., Diamanti, E., Pizzirani, D., Tardia, P., Maccesi, M., Realini, N., Magotti, P., Garau, G., Bakkum, T., Rivara, S., Mor, M. & Piomelli, D. Synthesis and characterization of the first inhibitor of *N*-acylphosphatidylethanolamine phospholipase D (NAPE-PLD). *Chemical Communications* **53**, 12814-12817 (2017).
12. Eder, J., Sedrani, R. & Wiesmann, C. The discovery of first-in-class drugs: origins and evolution. *Nature Reviews Drug Discovery* **13**, 577 (2014).
13. Macarron, R., Banks, M.N., Bojanic, D., Burns, D.J., Cirovic, D.A., Garyantes, T., Green, D.V.S., Hertzberg, R.P., Janzen, W.P., Paslay, J.W., Schopfer, U. & Sittampalam, G.S. Impact of high-throughput screening in biomedical research. *Nature Reviews Drug Discovery* **10**, 188 (2011).
14. Inglese, J., Johnson, R.L., Simeonov, A., Xia, M., Zheng, W., Austin, C.P. & Auld, D.S. High-throughput screening assays for the identification of chemical probes. *Nature Chemical Biology* **3**, 466 (2007).
15. Peppard, J.V., Mehdi, S., Li, Z. & Duguid, M.S. WO 2008/150832 A1.
16. Karawajczyk, A., Orrling, K.M., de Vlieger, J.S.B., Rijnders, T. & Tzalis, D. The European Lead Factory: a blueprint for public–private partnerships in early drug discovery. *Frontiers in Medicine* **3** (2017).
17. Schmid, P.C., Reddy, P.V., Natarajan, V. & Schmid, H.H. Metabolism of *N*-acylethanolamine phospholipids by a mammalian phosphodiesterase of the phospholipase D type. *Journal of Biological Chemistry* **258**, 9302-9306 (1983).
18. Natarajan, V., Schmid, P.C., Reddy, P.V. & Schmid, H.H.O. Catabolism of *N*-Acylethanolamine phospholipids by dog brain preparations. *Journal of Neurochemistry* **42**, 1613-1619 (1984).
19. Ueda, N., Liu, Q. & Yamanaka, K. Marked activation of the *N*-acylphosphatidylethanolamine-hydrolyzing phosphodiesterase by divalent cations. *Biochimica et Biophysica Acta (BBA) - Molecular and Cell Biology of Lipids* **1532**, 121-127 (2001).
20. Wang, J., Okamoto, Y., Morishita, J., Tsuboi, K., Miyatake, A. & Ueda, N. Functional analysis of the purified anandamide-generating phospholipase D as a member of the metallo-β-lactamase family. *Journal of Biological Chemistry* **281**, 12325-12335 (2006).
21. Wang, J., Okamoto, Y., Tsuboi, K. & Ueda, N. The stimulatory effect of phosphatidylethanolamine on *N*-acylphosphatidylethanolamine-hydrolyzing phospholipase D (NAPE-PLD). *Neuropharmacology* **54**, 8-15 (2008).
22. European Lead Factory assay requirements: https://www.europeanleadfactory.eu/how-submit/drug-target-assays/requirements.

23. Baggelaar, M.P., Janssen, F.J., van Esbroeck, A.C.M., den Dulk, H., Allarà, M., Hoogendoorn, S., McGuire, R., Florea, B.I., Meeuwenoord, N., van den Elst, H., van der Marel, G.A., Brouwer, J., Di Marzo, V., Overkleeft, H.S. & van der Stelt, M. Development of an activity-based probe and *in silico* design reveal highly selective inhibitors for diacylglycerol lipase-α in brain. *Angewandte Chemie International Edition* **52**, 12081-12085 (2013).
24. Baggelaar, M.P., Chameau, P.J.P., Kantae, V., Hummel, J., Hsu, K.L., Janssen, F., van der Wel, T., Soethoudt, M., Deng, H., den Dulk, H., Allara, M., Florea, B.I., Di Marzo, V., Wadman, W.J., Kruse, C.G., Overkleeft, H.S., Hankemeier, T., Werkman, T.R., Cravatt, B.F. & van der Stelt, M. Highly selective, reversible inhibitor identified by comparative chemoproteomics modulates diacylglycerol lipase activity in neurons. *J. Am. Chem. Soc.* **137**, 8851-8857 (2015).
25. van der Wel, T., Janssen, F.J., Baggelaar, M.P., Deng, H., den Dulk, H., Overkleeft, H.S. & van der Stelt, M. A natural substrate-based fluorescence assay for inhibitor screening on diacylglycerol lipase α. *Journal of Lipid Research* **56**, 927-935 (2015).
26. Navia-Paldanius, D., Savinainen, J.R. & Laitinen, J.T. Biochemical and pharmacological characterization of human α/β-hydrolase domain containing 6 (ABHD6) and 12 (ABHD12). *Journal of Lipid Research* **53**, 2413-2424 (2012).
27. Soethoudt, M., Grether, U., Fingerle, J., Grim, T.W., Fezza, F., de Petrocellis, L., Ullmer, C., Rothenhäusler, B., Perret, C., van Gils, N., Finlay, D., MacDonald, C., Chicca, A., Gens, M.D., Stuart, J., de Vries, H., Mastrangelo, N., Xia, L., Alachouzos, G., Baggelaar, M.P., Martella, A., Mock, E.D., Deng, H., Heitman, L.H., Connor, M., Di Marzo, V., Gertsch, J., Lichtman, A.H., Maccarrone, M., Pacher, P., Glass, M. & van der Stelt, M. Cannabinoid CB_2 receptor ligand profiling reveals biased signalling and off-target activity. *Nature Communications* **8**, 13958 (2017).

Supplementary Information

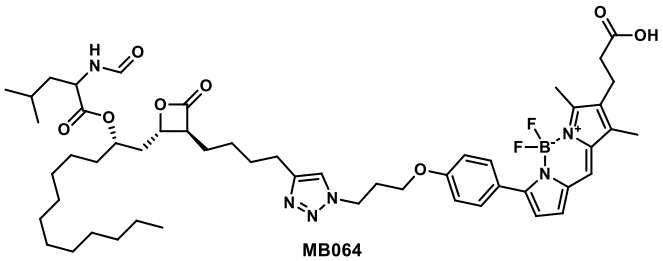

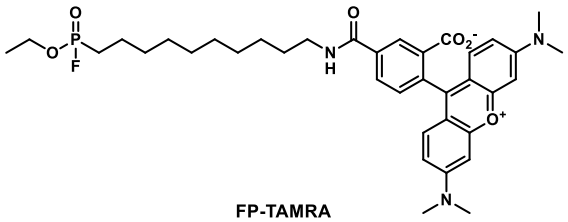

Supplementary Figure 1. Structures of serine hydrolase activity-based probes MB064[23] and FP-TAMRA.